Pergamon

SCIENCE DIRECT®

Tetrahedron 59 (2003) 8365–8374

TETRAHEDRON

Aromatic δ-peptides: design, synthesis and structural studies of helical, quinoline-derived oligoamide foldamers

Hua Jiang,[a] Jean-Michel Léger,[b] Christel Dolain,[a] Philippe Guionneau[c] and Ivan Huc[a,*]

[a]*Institut Européen de Chimie et Biologie, 16 av. Pey Berland, 33607 Pessac Cedex, France*
[b]*Laboratoire de Pharmacochimie, Université Victor Segalen Bordeaux II, 146 rue Léo Saignat, 33076 Bordeaux, France*
[c]*Institut de Chimie de la Matière Condensée de Bordeaux, 87 Avenue du Docteur Schweitzer, 33608 Pessac Cedex, France*

Received 6 June 2003; revised 1 August 2003; accepted 29 August 2003

Abstract—Oligoamides of 8-amino-4-isobutoxy-2-quinolinecarboxylic acid were designed and synthesized, and their helical structures were characterized in the solid state by single crystal X-ray diffraction, and in solution by ^{1}H NMR. The monomer methyl 4-isobutoxy-8-nitro-2-quinolinecarboxylate is easily prepared in three steps from 2-nitroaninile and dimethyl acetylene dicarboxylate. Successive hydrogenations of nitro groups, saponifications of esters and couplings of amines and acids via the acid chlorides gave a dimer, tetramer, hexamer, octamer, and decamer in a convergent fashion. The oligomers were shown to adopt a bent conformation stabilized by intramolecular hydrogen bonds between amide hydrogens and adjacent quinoline nitrogens. In the solid, the dimer adopts a planar crescent shape and the octamer a helical conformation. All NMR data are consistent with similar conformations in solution. The helices are apparently remarkably stable. Some of them remain helical even at 120°C in deuterated DMSO. The structural studies confirm the predictions made by computer and demonstrate the high potency of the design principles.

1. Introduction

Numerous small and large peptides have biological activities that could have useful therapeutic applications if they were not readily degraded in vivo by proteases. For many years, chemists have worked at the design of so called peptidomimetics: protease resistant unnatural substances mimicking the structures and potentially the functions of peptides. Whilst initial studies were focused on analogues of relatively small peptides, recent developments have demonstrated that the folded secondary structures of large peptides (e.g. α-helices or β-sheets, or β-turns) can also be mimicked by unnatural oligomers. Such oligomers having predictable and well-defined conformations in solution are termed foldamers.[1–3] They represent a significant step forward in the field of peptidomimetics and, in the long run, may open the door to fully synthetic analogues of proteins.

The most studied families of unnatural oligomers mimicking the folded structures of α-peptides are aliphatic in nature.[2,3] They comprise β-, γ-, and δ-homologues of peptides, assembled using various linkages such as amides, sulfonamides, sulfoximine, *N*-oxo-amides, ureas, or hydrazides.[3–5] Several families of aromatic oligomers have also been shown to adopt stable linear, bent, and helical conformations that may prove useful in the field of peptidomimetics.[3,6–15] Among these, the aromatic structures which bear the strongest analogy with peptides are oligoamides as well, the conformation of which can be stabilized by hydrogen bonds between amide groups and donors or acceptors belonging to the adjacent aromatic rings. Several families of aromatic oligoamides have been described based on various aromatic building blocks (e.g. pyridines,[6–9] anthranilic acids,[6,7] pyridine oxides,[6] pyrazines,[10] 1,3-dimethoxybenzenes[7,11]…). Some aromatic oligomers have also been based on ureas[12] or hydrazides[13] instead of amide linkages, and others have been incorporated into aliphatic sequences in order to template their structures.[14] Overall, these aromatic oligomers have been less studied than their aliphatic counter-parts despite the fact their specific features should be very useful in the context of applications.[15] For example, they often exhibit high conformational stability and very strong resistance to hydrolysis (as aromatic amides in general), and most importantly their structures can often be accurately predicted.

In the following, through the presentation of the synthesis and structural studies of a new family of quinoline derived oligomers,[16] we aim to emphasize the efficiency and generality of simple design principles of aromatic oligoamide foldamers.

Keywords: heterocycles; conformation analysis; helical structures; hydrogen bonds; supramolecular chemistry.
* Corresponding author. Tel.: +33-540-00-22-19; fax: +33-540-00-22-26; e-mail: i.huc@iecb-polytechnique.u-bordeaux.fr

0040–4020/$ - see front matter © 2003 Elsevier Ltd. All rights reserved.
doi:10.1016/j.tet.2003.08.058

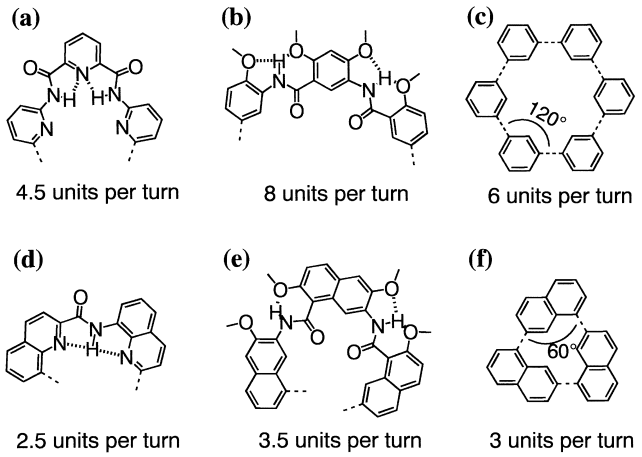

Figure 1. Bending of aromatic oligomers depends on intramolecular hydrogen bonds on the inner or outer rim of the oligomer, and on the substitution motif (*ortho*, *meta*…) of aromatic rings.

2. Design of the structures

The predictability of the folding of an oligomeric molecule is largely increased when stabilizing intramolecular interactions (e.g. hydrogen bonds) take place between consecutive units. The computational and/or experimental studies of a simple dimer or trimer then provides accurate data on the relative positioning of consecutive units that, in many cases, may be extrapolated to longer oligomers. Good illustrations of this strategy are oligoamides derived from pyridine diamines and pyridine diacids (Fig. 1(a)),[8,9] or those derived from 4,6-dimethoxy-3-amino-benzoic acid (Fig. 1(b)).[11] Short oligomers in these series adopt planar 'crescent' conformations stabilized by intramolecular hydrogen bonds between consecutive units. Longer oligomers are bent in the same way, and slightly deviate from planarity so as to form helices. In contrast, the conformational study of a dimeric, trimeric, or tetrameric α-peptide give little indication that longer sequences may fold into an α-helix.

The pitch of aromatic oligoamide helical foldamers typically corresponds to the thickness of one aromatic ring. This parameter is fixed and does not allow to tune the structures. On the other hand, the diameter of the helices and the number of monomers per helical turn depend directly on the relative positioning of consecutive units. In oligomers of six-membered *meta* substituted aromatics, one expects an angle of approximately 120° between consecutive units leading to about six units per helical turn (Fig. 1(c)). In practice, intramolecular hydrogen bonding has an effect on the bending of the strands. In the case of oligomers of pyridine diamines and pyridine diacids (Fig. 1(a)), the hydrogen bonds take place at the inner rim of the helices, which pinches the strand and reduces the number of monomer per turn to approximately 4.5. Conversely, when the hydrogen bonds take place at the outer rim of the helices, the bending of the strand is reduced and about 8 units are necessary to accomplish one turn (Fig. 1(b)).

In any case, bending remains larger than in helices of aliphatic α, β and γ peptide for which 2 to 4 units per turn is typical. We speculated that aromatic oligoamides with substituents oriented at 60° (for example *ortho* substituents), may be more bent and give rise to helices with approximately 3 units per turn (Fig. 1(f)). Quinoline monomer **1c** was designed for this purpose (Scheme 1). Its nitro and ester groups can respectively, be reduced to an amine and saponified to an acid, oriented at ~60°. It possesses an endocyclic nitrogen that should allow intramolecular hydrogen bonding with adjacent amide hydrogens (Fig. 1(d)), and the isobutoxy substituent in position 4 is expected to diverge from the helix and tune its solubility. Molecular modeling (see below) supports these predictions and suggests a helical conformation for strands as short as a trimer. Conversely, modeling shows that about 3.5 units should be necessary to accomplish one turn using a similar substitution motif, but when hydrogen bonds take place on the outer rim (Fig. 1(e)).

3. Synthesis

The preparation of monomer **1c** was easily carried out in three steps (Scheme 1). As described in the literature,[17] the addition of 2-nitro-aniline to dimethyl acetylene dicarboxylate gives **1a** which can be isolated by simple filtration (yield >70%). An X-ray structure of this compound allowed to assign a *trans* configuration of the double bond (Fig. 2). The conversion of enamine **1a** to quinolinone **1b** can be carried out either thermally (reflux of Ph_2O) or in PPA (yield about 65%).[17] The quinolinone tautomeric form of **1b** in the solid state was characterized by single crystal X-ray diffraction (Fig. 2). The alkylation of the oxygen in position 4 was achieved under Mitsunobu conditions in 90% yield. The structure of the product was again validated by an X-ray structure (Fig. 2). No trace of *N*-alkylation was detected in this reaction. Hydrogenation and saponification of nitro-ester **1c** under standard conditions gave quantitative yields of amino-ester **1d** and nitro-acid **1e**, respectively. The activation of **1e** proceeded smoothly in refluxing $SOCl_2$ and the subsequent reaction with **1d** gave nitro-ester dimer **2a** in excellent yield.

The hydrogenation, saponification, activation in $SOCl_2$ and coupling were applied successfully to dimer **2a** to give

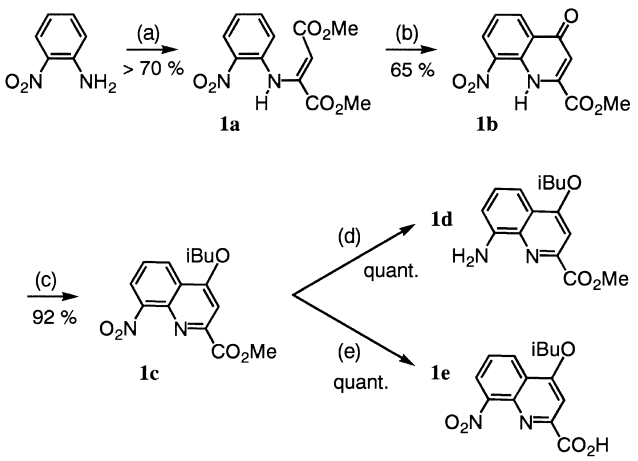

Scheme 1. Synthesis of quinoline monomers: (a) dimethylacetylene dicarboxylate, MeOH, △; (b) PPA, 120°, or diphenyl ether, reflux; (c) *i*BuOH, DIAD, PPh_3, THF, rt; (d) H_2–Pd/C, EtOAc, rt; (e) KOH, THF–water 2:1 vol/vol.

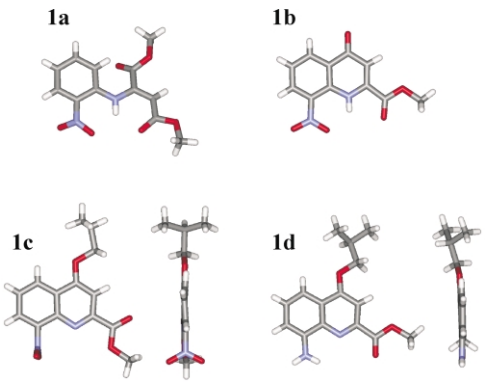

Figure 2. Stick representations of the structures of **1a**–**1d** in the crystal.

tetramer **4a**, and again to tetramer **4a** to give hexamer **6a** and octamer **8a** (Scheme 2). When the reactions are performed on larger scales, the yields tend to be higher. The possibility to double the size of the oligomer at each step, or 'segment doubling strategy',[18] may lead very effectively to long structures and high molecular weights. However, we observed that the hydrogenation and the saponification steps require increasing reaction times and/or higher temperatures as the length of the oligomers increases. This is presumably due to the folding of the structures in the reaction mixtures, which hinder the reactive functions. When the activation of octamer acid **8c** and its coupling to octamer amine **8b** was attempted, only minor quantities of hexadecamer were detected (<10%). This very low yield may be attributed partly to the fact the reaction was performed on a very small scale, and partly to a slow reaction rate. Thus, the convergent synthesis of very long strands will require some improvement, maybe using larger scales, longer reaction times or higher temperatures.

In the meantime, we showed that long strands can be prepared using an iterative approach. The coupling reactions work well when one of the reagents has a folded structure and the other is short and unhindered. For example, amine **8b** reacts with the acid chloride of dimer **2c**, to give decamer **10a** (Scheme 2), which in turn may serve as a precursor of a dodecamer and so on. Though less efficient than a convergent segment doubling strategy, this iterative approach should be useful to incorporate a series of different monomers in a sequence, as in solid-phase peptide synthesis.

4. Solid state structural studies

The solid state structures of precursors **1a** and **1b**, of monomers **1c** and **1d**, of dimer **2a**, and of octamer **8a**[16] were all characterized by single crystal X-ray diffraction analysis. The crystallographic data are summarized in Table 1. The structures of **1a**–**1d** give useful information about their conformational and tautomeric preferences (Fig. 2). In enamine **1a**, the amine proton is involved in two hydrogen bonds defining two six-membered hydrogen-bonded rings. One hydrogen bond involves a nitro oxygen (NH···ON: 2.64 Å, 142.6°)[19] and the other a carbonyl oxygen (NH···O=C: 2.73 Å, 124.7°).[19] The nitro group is almost

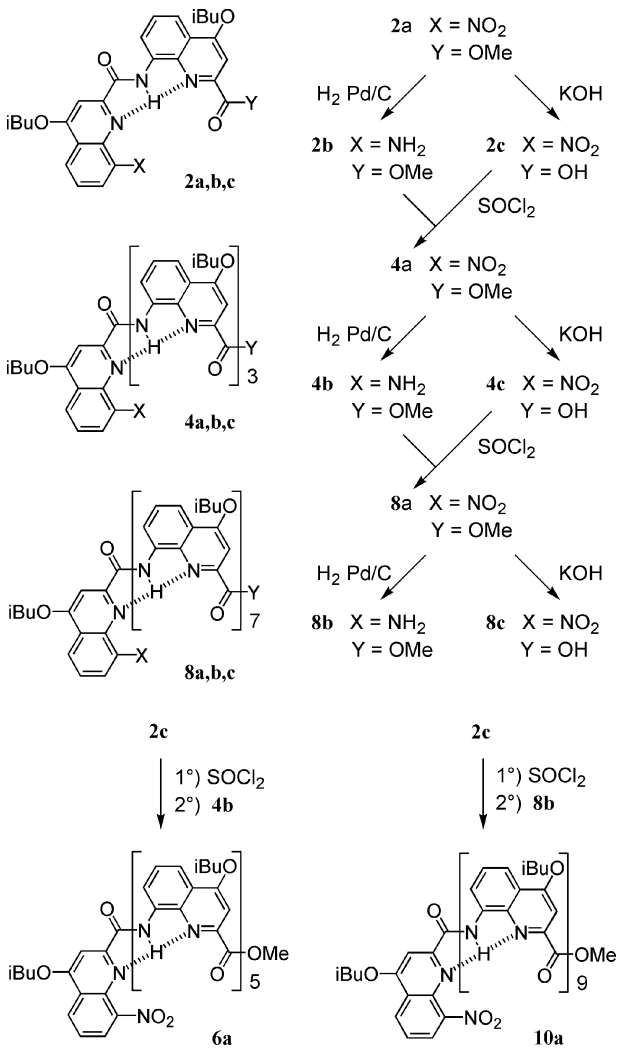

Scheme 2. Synthesis of quinoline oligoamides. Hydrogenations and saponifications are quantitative. Coupling yields range from 29 to 97%.

in the plane of the phenyl ring (torsion angle 26.1°). Interestingly, the carbonyl carbon nearest to the phenyl ring is not the one involved in the electrophilic substitution which gives **1b**.

The structure of **1b** is that of a 4-(1*H*)-quinolinone. The electron density of a proton can be refined on the quinoline nitrogen, and the C–O distance in position 4 is that of a double bond (1.26 Å, as opposed to 1.36 Å in **1c** and **1d**). As for compound **1a** the proton in position 1 is involved in two hydrogen bonds. A hydrogen bond with a nitro oxygen (NH···ON: 2.62 Å, 129.5°)[19] defines a six-membered hydrogen-bonded ring, and a hydrogen bond with the ester carbonyl oxygen (NH···O=C: 2.66 Å, 105.4)[19] defines a five-membered hydrogen-bonded ring. The nitro group is in the plane of the phenyl ring (torsion angle 3.6°).

Compound **1c** contains no hydrogen available for intramolecular hydrogen bonding. Its structure reveals the repulsions between the different hydrogen bond acceptors of the molecule. Because of the repulsion between the quinoline oxygen and the nitro oxygens, the nitro group is found almost perpendicular to the aromatic ring (torsion angle of 94°6). The ester group remains in the plane of the

Table 1. Crystallographic parameters for the structures determined by X-ray diffraction analysis

Compound	**1a**	**1b**	**1c**	**1d**	**2a**
M_w	$C_{12}H_{12}N_2O_6$	$C_{11}H_8N_2O_5$	$C_{15}H_{16}N_2O_5$	$C_{15}H_{18}N_2O_3$	$C_{29}H_{30}N_4O_7$
Crystallizing solvent/precipitant	$CHCl_3$/*n*-hexane	Toluene/*n*-hexane	Toluene/*n*-hexane	Toluene/air	Nitrobenzene/*n*-hexane
Crystal dimensions (mm)	0.40×0.40×0.15	0.30×0.15×0.10	0.25×0.32×0.50	0.35×0.35×0.25	0.45×0.45×0.40
Color	Yellow	Yellow	Yellow	Colorless	Yellow
Radiation type	Cu K_α	Cu K_α	Cu K_α	Cu K_α	Mo K_α
Unit cell	Monoclinic	Monoclinic	Orthorombic	Monoclinic	Monoclinic
Space group	*P*21/*n*	*P*21/*n*	*Pna*21	*P*21/*c*	*P*21/*n*
a (Å)	9.299(4)	11.1580(10)	10.012(1)	7.713(1)	10.497(1)
b (Å)	10.495(3)	5.3940(10)	22.741(4)	10.589(4)	21.402(1)
c (Å)	13.640(3)	17.559(2)	6.875(1)	17.822(1)	12.295(1)
β (°)	97.07(3)	93.08(10)	90	102.16(3)	92.68(1)
V ($Å^3$)	1321.0(7)	1055.3(2)	1565.3(4)	1422.9(6)	2759.1(4)
Z	4	4	4	4	4
FW (g mol^{-1})	280.24	248.19	304.30	274.31	546.57
ρ (g cm^{-3})	1.409	1.562	1.291	1.280	1.316
Scanned θ	$5.33 \leq \theta \leq 64.86$	$4.59 \leq \theta \leq 59.92$	$4.83 \leq \theta \leq 64.89$	$6.58 \leq \theta \leq 64.94$	$3.23 \leq \theta \leq 27.46$
Total/unique refl.	2222/2222	1528/1528	1428/1428	2408/2408	15357/5997
Parameters	182	164	191	182	362
GOF	1.074	1.123	1.017	1.182	1.042
*R*1 (%)	6.2	4.1	8.15	5.47	6.99
CCDC Ref.	211432	211434	211436	211435	211433

aromatic ring, but the carbonyl is pointing away from the quinoline nitrogen. This structure also reveals that the carbon of the CH_2 group of the isobutoxy moiety is in the plane of the quinoline ring, *anti* to C(10) and *syn* to C(3). This conformation is conserved in all 4-isobutoxy quinolines we have characterized in the solid state. It is presumably due to steric repulsions between the CH_2 protons and the proton in position 5 of the quinoline.

The X-ray structure of **1d** shows that the amino group, unlike the nitro group from which it is derived, lies in the plane of the aromatic ring, forming a hydrogen bond with the quinoline nitrogen (NH···N: 2.69 Å, 104.0°). As shown in Figure 3, the same hydrogen bond is present in the structure of dimer **2a** (NH···N: 2.69 Å, 108.4°). The amide proton is also hydrogen bonded to the other quinoline nitrogen (NH···N: 2.72 Å, 126.5°). These two hydrogen bonds set the relative orientation of the quinoline rings in a crescent conformation, as expected initially. The torsion angles within the backbone of the molecule are all inferior to 4°, indicating that aromatic and amide moieties are almost perfectly coplanar. The nitro and ester groups slightly deviate from this plane.

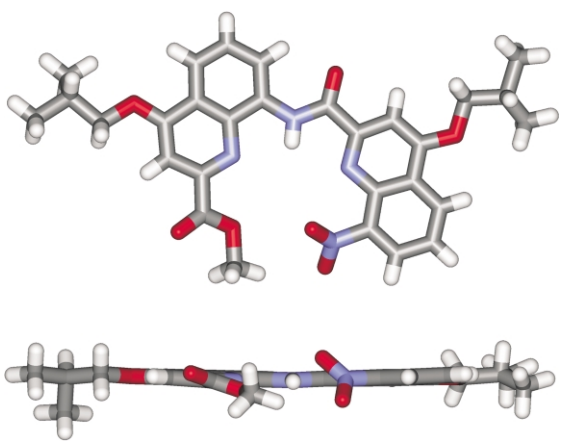

Figure 3. Front view and side view of the structure of **2a** in the crystal.

The bending of dimer **2a** allows us to speculate that a trimer cannot adopt a fully planar conformation, and that a steric clash between the extremities of the strand will force a torsion into a right handed or a left handed helix. This was confirmed by the X-ray structure of **8a** (Fig. 4)[16] which shows a helix extending to more than three turns. The third unit in the octamer indeed overlaps with the first one. The pitch of the helix is identical to the pitch of other helical aromatic oligoamides and corresponds to the thickness of one aromatic ring (3.4 Å). The inner rim of the helix accomplishes approximately one turn every 15 main chain atoms and adopts a conformation similar to that of a pentaaza-15-crown-5 macrocycle, with alternating amido and pyrido nitrogens. Thus, almost exactly five units are required for two helical turns (equivalent to 30 atoms of the inner rim), which corresponds to the highest curvature reached by helical aromatic oligoamides until now. Consequently, helices of quinoline derived **4a**–**10a** also have the largest length per number of units: the helix of **8a** is about 13 Å long, compared to 6.8 Å for octamers of pyridine oligoamides. The amido protons fill the helix hollow, and completely prevent penetration of solvent molecules. As in the dimer, amide protons are all involved in two hydrogen bonds with the adjacent quinoline nitrogens that set the orientation of the amido and quinoline moieties (Fig. 1). The relative inclination of consecutive units can be estimated from the torsion angles between the N(1)–C(2) bond of a quinoline and the C(8)–C(9) of the next quinoline which range from 159.2 to 169.5°. The isobutyl chains adopt various conformations, but the position of the CH_2 carbon is always the one found in the monomers **1c** and **1d**. The core of the helix has a very regular structure, illustrated by almost constant distances between the oxygens in position 4 of the quinolines (from 11.87 to 11.93 Å). Bending is even along the strand and does not depend upon the central or terminal position of the units, or the conformation of the side chain or interactions associated with crystal packing.

The principles used to design the folded conformation of

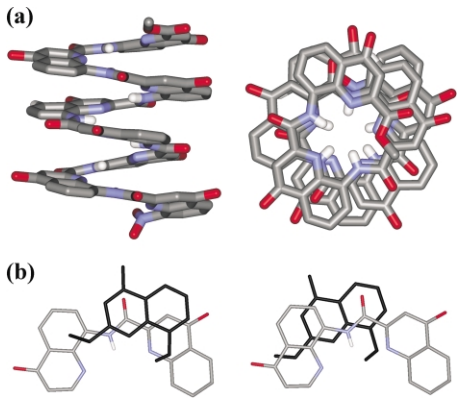

Figure 4. Crystal structure of **8a**. Included solvent molecules, hydrogens, and isobutyl chains have been omitted for clarity. (a) Side view and top view of the entire structure; (b) fragments showing the relative positioning of quinoline rings (in black) above and below a quinoline dimer within the helix. The direction of these views is perpendicular to the planes of the aromatic rings, and not exactly parallel to the helix axis. Consequently, the two quinolines in black appear as off-set whislt they are almost superimposed in the structure.

these oligomers are essentially based on the hydrogen bonds between consecutive units within the sequence. However, the solid state structure shows extensive aromatic overlap which probably plays an important role in the stabilization of the helix. As shown in Figure 4(b), a given quinoline in the helix does not have the same position with respect to the aromatic rings above it and below it. Computational methods may provide an estimate of the strength of interactions between these stacked aromatics. But a simple comparison of the structure of **8a**, where intramolecular aromatic stacking is extensive, and of **2a**, where there is no intramolecular stacking, already provides useful information. As shown in Figure 5, the structure of **2a** matches very well with the N-terminal fragment of the structure of **8a**. This suggests that the curvature of the strands is essentially determined by the hydrogen-bonds. Intramolecular aromatic stacking in **8a** either happens to be optimum in the position set by hydrogen-bonding, or provides too small a gain in interaction energy to perturb the hydrogen bonds and force the curvature to change to the position where it is most favorable. Thus, the fact that we neglect aromatic stacking apparently has little consequence on the accuracy of the design. In oligoamide aromatic foldamers, it may in principle be possible to study a simple dimer and extrapolate its structure to predict the helix formed by a longer oligomer.

The crystal structure of **8a** also allows us to rate the quality of the prediction made by very simple molecular modeling methods. Figure 6 shows the superposition of the helix of **8a** in the solid state, and the helix predicted for **8a** by an energy minimization using the MM3 force field in Macromodel, without changing anything to the set of parameters available. A side view of the helix shows an almost perfect prediction of its diameter and of its pitch. Top views show that when the N-terminal regions are docked so as to match, the C-terminal regions are offset by less than 3 Å after three helical turns. This indicates that the prediction of the curvature of the helix (the number of units per turn) is not perfect, but that the error remains below 5%.

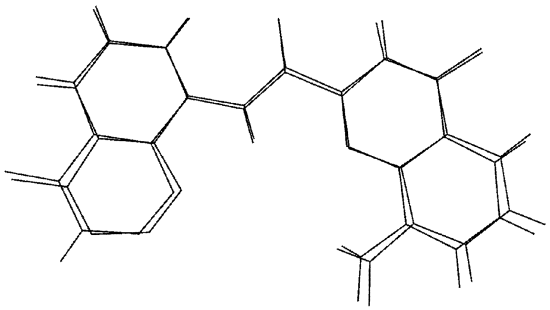

Figure 5. Superposition of part of the structure of **2a** in the crystal and the N-terminal fragment of the structure of **8a** in the crystal. In **2a**, the dihedral angles of the linkages between the amide and both quinoline rings have been changed so as to match those of **8a**.

5. Solution studies

Solution studies were performed to assess whether the folded structures observed in the solid state are also prominent in solution. The ^{1}H NMR spectra of **2a**–**10a** in $CDCl_3$ are sharp (Fig. 7) and show no indication of hybridization into double helices or other types of aggregates, as was observed for pyridine derived oligoamides.[9] The signals are spread over a remarkably large range of chemical shifts despite the repetitive nature of the sequences, suggesting different environments of the units. Amide protons are deshielded at 10–12.5 ppm, as expected for a hydrogen-bonded structure. Increasing strand length results in a strong shielding of aromatic, amide and ester protons that can be attributed to tight contacts between aromatic rings. For example, the signal of the ester CH_3 shifts from 4.23 ppm in **2a** to 2.93 ppm in **10a** (Fig. 7), and the singlets assigned to the protons in position 3 of the quinoline are found between 7.63 and 8.01 ppm in **2a**, and between 6.05 and 6.96 ppm in **10a**. On the other hand, the chemical shifts of the isobutyl residues are relatively independent from oligomer length.

The UV–vis absorption spectra of **2a**–**10a** show bathochromic and hypochromic effects with increasing oligomer length which also suggest intramolecular π-stacking in solution. The spectrum of **2a** is characterized by an absorption maximum at 245 nm (ε=40400 mol^{-1} L cm^{-1}), and by a broad series of less intense bands from 300 to 430 nm ($\varepsilon\approx$12000 mol^{-1} L cm^{-1}). As the strands become longer, these absorption maxima are red-shifted up to $\Delta\lambda$=8 nm, and the molar extinction coefficients 'per

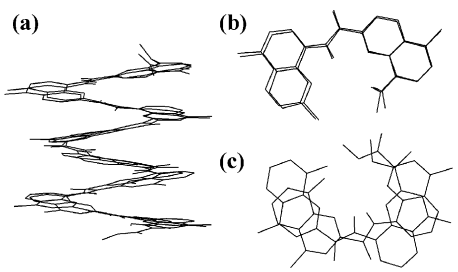

Figure 6. Superposition of the structures of **8a** in the crystal and obtained from a simple energy minimization (MM3 force field in Macromodel). (a) Side view of the helix; (b) top view of the N-terminal fragments which were positioned so as to result in the best match; (c) superposition of the C-terminal fragments which show an offset of about 3 Å of the helices.

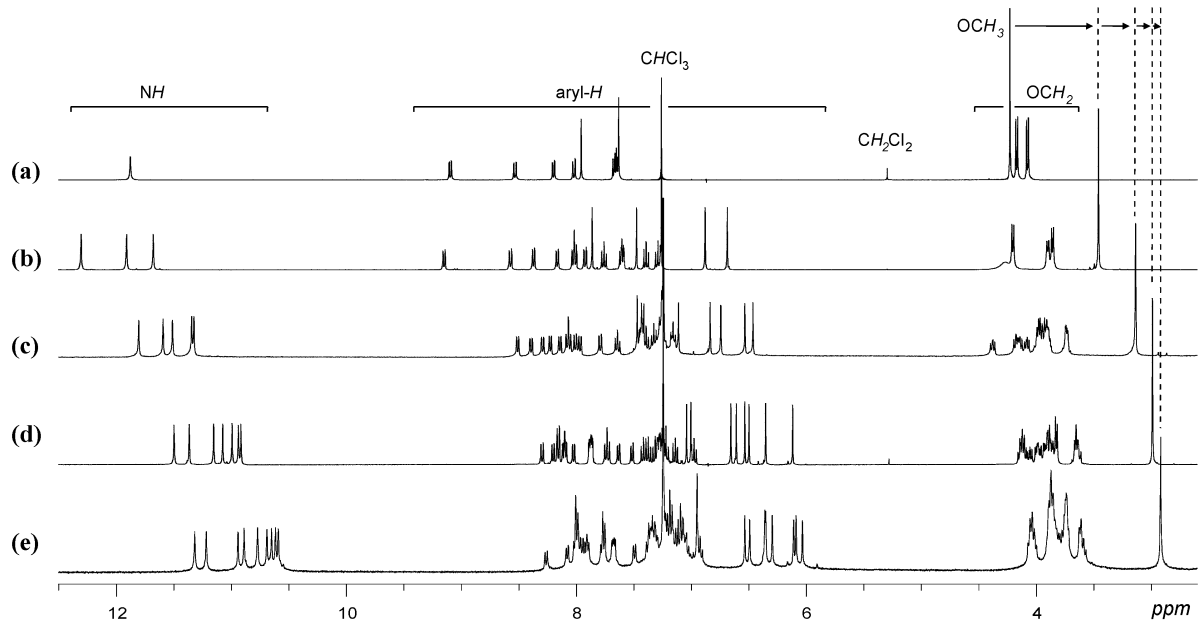

Figure 7. Part of the ^{1}H 400 MHz NMR spectra of: (a) **2a**; (b) **4a**; (c) **6a**; (d) **8a**; and (e) **10a** in $CDCl_3$.

quinoline ring' drop by 20–25%. In all these oligomers, the fluorescence of the quinolines is quenched, presumably by the nitro groups.

Upon adding chiral shift reagent Eu(hfc)$_3$ to a $CDCl_3$ solution of **8a**, amide, aromatic and ester ^{1}H NMR signals split into two signals of equal intensities, suggesting that this compound exists as a mixture of enantiomers, and that stereoselective interactions with Eu(hfc)$_3$ do not induce an enantiomeric excess. This is also supported by the pattern of the signals of the OCH_2 groups at 3.4–4.4 ppm. In the absence of Eu(hfc)$_3$, these signals appear as sharp doublets in **2a** and as diastereotopic motifs in **6a**, **8a**, and **10a**. For tetramer **4a**, three OCH_2 doublets are seen along with a broad signal. Upon heating this broad signal sharpens into a doublet, and upon cooling, all signals coalesce before sharpening into doublets of doublets (Fig. 8). This compound adopts a chiral conformation as well, but its inversion is faster. For comparison, inversions of **8a** and **6a** are slow even at high temperatures in polar solvents. For example no coalescence is observed at 120°C in D_6-DMSO (!) although the chemical shift differences between the signals of diastereotopic protons are similar to those of **4a** in $CDCl_3$, and despite the fact that DMSO should compete with intramolecular hydrogen bonding and destabilize the helices to some extent.

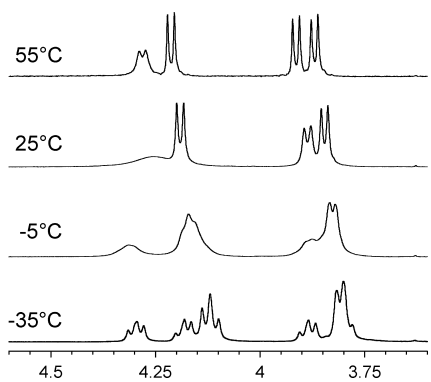

Figure 8. Part of the ^{1}H 400 MHz NMR spectra of **4a** in $CDCl_3$ at various temperatures showing the emergence of diastereotopic patterns in the signals of CH_2 groups.

These data are similar to the data obtained for oligoamides of 2,6-pyridinedicarboxylic acids and 2,6-diaminopyridines. They are consistent with helical structures of **4a**, **6a**, **8a** and **10a** in solution, but do not fully demonstrate that the solution conformations are identical to those observed in the solid state. ROESY experiments on **8a** show correlations between protons in position 3 of the quinolines and protons in position 5 and 7. We expect that these correlations will give direct evidence of a helical structure in solution but we have failed up to now in assigning these signals unambiguously to the corresponding quinoline rings in the sequence. The NMR techniques developed for solving the solution structures of α-peptides have been applied to aliphatic β- and γ-peptides but are not directly applicable to aromatic compounds.[20] In particular, the string of spin systems on the sequence cannot be reconstituted solely from correlations between protons, and requires the assignment of a large part of the ^{13}C NMR spectrum. We are currently working on NMR protocols that should allow complete assignment and solution of the structure of aromatic amide oligomers.

Assuming that the helices in solution are indeed like the helix observed in the solid state by single crystal X-ray diffraction, the relative rates of helix inversion of **4a**, **6a**, and **8a** are particularly remarkable. The temperature of coalescence of the signals of the diastereotopic CH_2 protons is below 25°C for **4a**, and well above 120°C for **6a** and **8a**, since at that temperature, the signals are barely broader than at 25°C. This implies that the helical shape is almost fully conserved even at high temperature and suggests that the helices of **6a**–**10a** are considerably more stable than most, if not all, folded helical oligomers of similar lengths reported up to now.

Because **4a** is shorter than two turns, its inversion can, in principle, proceed through a rotation of ca. 330° about a single bond connected to the central amide group. The activation of this process requires the disruption of a single hydrogen bond, and of all intramolecular π−π contacts. On the other hand, oligomer **6a** is longer than two turns. Its inversion requires at least two simultaneous 330° rotations. The activation of this process thus requires the disruption of two hydrogen bonds and of all intramolecular π−π contacts. Although the length of **4a** and **6a** differ by only 30%, a significant difference in rates of inversion may indeed be expected, especially if intramolecular π−π stacking is cooperative. For strands longer than two turns (e.g. **8a** and **10a**), the inversion may proceed upon propagating along the structure a 5 or 6 units long unfolded segment connecting a stretch of right handed helix to a stretch of left handed helix. The formation and propagation of such a segment requires the simultaneous disruption of not more than two hydrogen bonds and of π−π stacking over not more than two helical turns.[21] Thus, the activation energy of helix inversion is not expected to increase as rapidly with strand length as if a full unfolding were necessary.

6. Conclusion

In summary, we have shown that very simple principles may allow the accurate design and prediction of the folding of oligomeric strands into stable helical structures. When the interactions, which stabilize the folded state occur between consecutive units, even an isolated dimer exhibits the pattern that leads to folding. The helical motif may be obtained by simply extrapolating the bent conformation of the shorter strands. The quinoline amino acid monomers we have presented are easily accessible, functionalizable, and assembled into oligoamides. These oligomers adopt unusually stable helical conformations even in polar solvents at high temperature. It seems reasonable to predict that water soluble versions of these oligomers (e.g. bearing polar groups in position 4) should fold just as well in aqueous medium. Such stable structures may represent attractive building blocks to elaborate synthetic mimics of tertiary structural motifs of proteins. Progress is currently made along these lines, and in the control of the helical handedness of these molecules.

7. Experimental

7.1. General

Solvents (THF, toluene, CH_2Cl_2) were dried by filtration over activated alumina on a commercially available setup. FTIR spectra were recorded on a Brucker IFS 55 FT-IR Spectrometer. 400 MHz ^{1}H and 100 MHz ^{13}C NMR spectra were recorded on a Brucker 400 Ultrashield spectrometer. The following notations are used for the ^{1}H NMR spectral splitting patterns: singlet (s), doublet (d), triplet (t), multiplet (m), broad (br). Melting points are uncorrected.

7.1.1. Methyl 4-isobutoxy-8-nitroquinoline-2-carboxylate 1c. A mixture of **1b**[17] (2 g, 8 mmol) and triphenylphosphine (2.25 g, 1.05 equiv.), 2-methyl-1-propanol (0.82 mL, 1.1 equiv.) and anhydrous THF (20 mL) under Argon, was cooled down to 0°C. Diisopropyl azodicarboxylate (1.71 mL, 1.05 equiv.) was added and the mixture was stirred at 0°C for 30 min, then at room temperature for 2 h. The solvent was evaporated and the product was purified by flash chromatography (SiO_2) eluting with CH_2Cl_2. Yield 2.25 g (92%) of a yellow solid. Mp: 174–175°C. ^{1}H NMR ($CDCl_3$) δ 8.47 (1H, dd, J=1.3, 6.7 Hz), 8.10 (1H, dd, J=1.3, 6.0 Hz), 7.63 (2H, m), 4.10 (2H, d, J=12.4 Hz), 4.04 (3H, s), 2.29 (1H, m), 1.14 (6H, d, J=6.7 Hz). ^{13}C NMR ($CDCl_3$) δ 165.62, 162.70, 151.22, 148.26, 139.94, 126.31, 125.87, 125.05, 123.24, 102.13, 75.56, 53.31, 28.05, 19.11. IR (KBr) ν, (cm^{-1}) 2963, 1721, 1591, 1568, 1533, 1471, 1441, 1424, 1366, 1329, 1269, 1244, 1124, 1016, 866, 787, 760. TOF-MS m/z: 305.19 $[M]^+$, 327.15 $[M+Na]^+$, 343.12 $[M+K]^+$.

7.1.2. Synthesis of amines 1d, 2b, 4b, 8b. General procedure for the hydrogenation of nitro groups. A mixture of the nitro precursor **1c**, **2a**, **4a** or **8a** (e.g. 8 mmol) dissolved in EtOAC (50 mL) and 10% Pd/C (0.29 g) was stirred at ambient temperature under a 4 bar atmosphere of hydrogen for 4 h. The solution was filtered through Celite, and the solvent was evaporated. The product was characterized by ^{1}H NMR and used without further purification.

Methyl 4-isobutoxy-8-aminoquinoline-2-carboxylate **1d**. Quantitative yield. Yellow solid. ^{1}H NMR ($CDCl_3$) δ 7.53 (1H, m), 7.48 (1H, s), 7.37 (1H, m), 6.95 (2H, dd, J=6.0, 1.3 Hz), 5.10 (2H, broad s), 4.02 (3H, m), 4.00 (2H, s), 2.27 (1H, m), 1.14 (3H, s), 1.12 (3H, s).

Dimer amine **2b** from nitro **2a**. Quantitative yield. Yellow solid. ^{1}H NMR ($CDCl_3$) δ 12.70 (1H, s), 9.04 (1H, m), 7.95 (1H, m), 7.76 (1H, s), 7.67 (1H, t, J=8 Hz), 7.56 (2H, m), 7.38 (1H, t, J=8 Hz), 7.02 (1H, m), 5.53 (2H, br), 4.10 (3H, s), 4.09 (2H, d, J=6.8 Hz), 4.06 (2H, d, J=6.8 Hz), 2.30 (2H, m), 1.16 (12H, m).

Tetramer amine **4b** from nitro **4a**. The temperature was raised to 50°C and the reaction time increased to 60 h. Quantitative yield. Yellow solid. ^{1}H NMR ($CDCl_3$) δ 12.44 (1H, s), 11.94 (1H, s), 11.81 (1H, s), 9.05 (1H, d, J=6.8 Hz), 8.43 (1H, d, J=7.2 Hz), 8.01 (3H, m), 7.87 (1H, d, J=8 Hz), 7.75 (1H, s), 7.73 (1H, t, J=8 Hz),7.64 (1H, t, J=8 Hz), 7.55 (1H, d, J=8 Hz), 7.32 (1H, s), 7.27 (1H, t, J=8 Hz), 7.02 (1H, t, J=8 Hz), 6.92 (1H, s), 6.68 (1H, s), 5.97 (1H, d, J=8.8 Hz), 4.19 (4H, m), 3.91 (2H, d, J=6.8 Hz), 3.87 (2H, d, J=6.8 Hz), 3.78 (2H, br), 3.52 (3H, s), 2.44 (2H, m), 2.33 (2H, m), 1.23 (24H, m).

Octamer amine **8b** from nitro **8a**. The temperature was raised to 50°C and the reaction time increased to 60 h. Quantitative yield. Yellow solid. ^{1}H NMR ($CDCl_3$) δ 11.56 (1H, s), 11.43 (1H, s), 11.34 (1H, s), 11.17 (1H, s), 11.08 (1H, s), 11.00 (1H, s), 10.93 (1H, s), 8.25 (1H, d, J=7.4 Hz), 8.12 (4H, m), 8.07 (1H, d, J=8.0 Hz), 7.89 (3H, m), 7.83 (1H, d, J=7.4 Hz), 7.73 (4H, m), 7.65 (1H, d, J=7.4 Hz), 7.45 (1H, t, J=8.0 Hz), 7.38 (1H, t, J=8.0 Hz), 7.30 (4H, m), 7.20 (1H, t, J=8.0 Hz), 6.99 (1H, t, J=8.0 Hz), 6.94 (1H, s), 6.88 (1H, s), 6.79 (1H, t, J=8.0 Hz), 6.68 (1H, s), 6.64 (1H, s), 6.53 (2H, s), 6.38 (1H, s), 6.18 (1H, s), 5.68

(1H, d, J=7.4 Hz), 4.13 (4H, m), 3.99 (4H, m), 3.85 (5H, m), 3.68 (2H, d, J=6.0 Hz), 3.61 (1H, m), 3.13 (2H, s), 3.01 (3H, s), 2.51 (2H, m), 2.31 (5H, m), 2.19 (1H, m), 1.36 (9H, m), 1.25 (30H, m), 1.11 (9H, m).

7.1.3. Synthesis of 1e, 2c, 4c, 8c. General method for the saponification of methyl esters. The methyl ester **1c**, **2a**, **4a**, or **8a** (e.g. 8 mmol) was dissolved in a mixture of THF (100 mL) and methanol (50 mL). KOH (2.5 equiv.) was added, and the solution was stirred at ambient temperature for 20 h. The solution was neutralized using excess AcOH and the product was extracted in dichloromethane (3×50 mL). The organic phase was washed with water, dried ($MgSO_4$) and evaporated to give a yellow solid which was characterized by ^{1}H NMR and used without further purification.

4-Isobutoxy-8-nitroquinoline-2-carboxyl acid **1e**, from ester **1c** (2.44 g). Quantitative yield. Yellow solid. ^{1}H NMR ($CDCl_3$) δ 8.56 (1H, dd, J=1.3, 6.0 Hz), 8.24 (1H, dd, J=1.3, 6.7 Hz), 7.74 (2H, m), 4.15 (2H, d, J=6.0 Hz), 2.33 (1H, m), 1.17 (3H, s), 1.15 (3H, s).

Dimer acid **2c** from ester **2a**. The reaction mixture was stirred at ambient temperature for 2 h. Quantitative yield. Yellow solid. ^{1}H NMR ($CDCl_3$) δ 11.72 (1H, s), 9.17 (1H, m), 8.56 (1H, d, J=8 Hz), 8.28 (1H, d, J=8 Hz), 8.08 (1H, d, J=8.8 Hz), 7.93 (1H, s), 7.79 (1H, s), 7.70 (2H, m), 4.19 (2H, d, J=6.4 Hz), 4.13 (2H, d, J=6.4 Hz), 2.32 (2H, m), 1.18 (3H, s), 1.17 (3H, s), 1.16 (3H, s), 1.15 (3H, s).

Tetramer acid **4c** from ester **4a**. The proportion of THF and methanol was adjusted to 9:1 vol/vol and the reaction mixture was stirred at 40°C for 2 h. Quantitative yield. Yellow solid. ^{1}H NMR ($CDCl_3$) δ 12.12 (1H, s), 11.66 (1H, s), 11.39 (1H, s), 9.15 (1H, d, J=6.8 Hz), 8.56 (1H, d, J= 8 Hz), 8.47 (1H, d, J=7.2 Hz), 8.14 (1H, d, J=7.2 Hz), 8.10 (1H, d, J=7.2 Hz), 8.02 (1H, d, J=8.8 Hz), 7.99 (1H, d, J=8 Hz), 7.95 (1H, s), 7.77 (1H, t, J=8 Hz), 7.63 (2H, m), 7.41 (2H, m), 7.29 (1H, t, J=8 Hz), 6.91 (1H, s), 6.77 (1H, s), 4.26 (4H, br), 3.91 (4H, m), 2.43 (4H, m),1.21 (24H, m).

Octamer acid **8c** from ester **8a**. The proportion of THF and methanol was adjusted to 9:1 vol/vol and the reaction mixture was stirred at 40°C for 8 h. Quantitative yield. Yellow solid. ^{1}H NMR ($CDCl_3$) δ 11.29 (1H, s), 11.17 (1H, s), 11.07 (1H, s), 10.99 (1H, s), 10.96 (1H, s), 10.95 (1H, s), 10.83 (1H, s), 8.32 (1H, d, J=8 Hz), 8.20 (2H, d, J=7.4 Hz), 8.16 (2H, m), 8.13 (1H, d, J=8.7 Hz), 8.05 (1H, d, J= 7.4 Hz), 7.88 (3H, t, J=8.7 Hz), 7.80 (2H, d, J=8.0 Hz), 7.66 (1H, d, J=8.0 Hz), 7.52 (1H, d, J=8.0 Hz), 7.42 (2H, m), 7.31 (4H, m), 7.15 (3H, m), 7.05 (1H, s), 7.01 (2H, m), 6.79 (1H, s), 6.66 (1H, s), 6.52 (1H, s), 6.47 (1H, s), 6.44 (1H, s), 6.15 (1H, s), 4.07 (3H, m), 3.89 (10H, m), 3.75 (2H, d, J=6.7 Hz), 3.65 (1H, t, J=7.4 Hz) 2.50 (3H, m), 2.32 (13H, m), 1.35 (8H, m), 1.20 (40H, m).

7.1.4. Synthesis of oligomers 2a, 4a, 6a, and 8a. General method for coupling an amine and an acid. A solution of the acid **1e**, **2c**, or **4c** (typically 1 mmol) in excess $SOCl_2$ was heated to reflux for 1 h. Most of the $SOCl_2$ was distilled off, and the remaining was azeotroped using anhydrous toluene (5 mL). The acid chloride was dissolved in anhydrous CH_2Cl_2 (5 mL), and added over a period of 10 min to a solution of amine **1d**, **2b**, **4b**, or **8b** (0.95 equiv.) and diisopropylethylamine (5.5 equiv.) in CH_2Cl_2 (10 mL) at 0°C. The reaction mixture was allowed to warm to room temperature and stirred overnight. The solvent was removed and the residue was purified by flash chromatography on silica gel eluting with EtOAc–toluene, from 2:98 to 10:90 vol/vol, to afford the pure product.

Dimer **2a**, from acid **1e** (1.5 g) and amine **1d** (1.44 g). Yield >96%. Yellow solid. Mp: 200–201°C. ^{1}H NMR ($CDCl_3$) δ 11.88 (1H, s), 9.10 (1H, dd, J=1.3, 6.7 Hz), 8.54 (1H, dd, J=1.3, 6.7 Hz), 8.21 (1H, dd, J=1.3, 6.7 Hz), 8.01 (1H, m), 7.96 (1H, s), 7.63 (3H, m), 4.23 (3H, s), 4.18 (2H, d, J=6.7 Hz), 4.08 (2H, d, J=6.7 Hz), 2.32 (2H, m), 1.16 (12H, m). ^{13}C NMR ($CDCl_3$) δ 166.89, 163.16, 162.71, 162.45, 153.93, 148.32, 147.80, 139.69, 139.34, 134.85, 127.78, 126.63, 125.37, 123.39, 122.25, 118.71, 116.65, 101.45, 100.23, 75.67, 75.14, 53.61, 28.16, 28.08, 19.21, 19.15. IR (KBr) ν, (cm^{-1}) 1718, 1671, 1593, 1567, 1522, 1418, 1341, 1109, 1038, 876, 749. TOF-MS m/z: 547.20 $[M]^+$, 569.16 $[M+Na]^+$, 585.13 $[M+K]^+$.

Tetramer **4a**, from acid **2c** (0.6 g) and amine **2b** (0.49 g). Yield 0.95 g (97%). Yellow solid. Mp: 208–210°C. ^{1}H NMR ($CDCl_3$) δ 12.30 (1H, s), 11.91 (1H, s), 11.68 (1H, s), 9.16 (1H, d, J=6.7 Hz), 8.58 (1H, d, J=6.7 Hz), 8.38 (1H, d, J=7.4 Hz), 8.15 (1H, d, J=6.7 Hz), 8.02 (2H, m), 7.93 (1H, d, J=7.4 Hz), 7.86 (1H, s), 7.76 (1H, t, J=8.0 Hz), 7.60 (2H, m), 7.47 (1H, s), 7.39 (1H, t, J=8.0 Hz), 7.27 (1H, t, J=8.0 Hz), 6.88 (1H, s), 6.69 (1H, s), 4.27 (2H, br), 4.20 (2H, d, J=6.7 Hz), 3.91 (2H, d, J=6.7 Hz), 3.85 (2H, d, J=6.7 Hz), 3.46 (3H, s), 2.49 (1H, m), 2.42 (1H, m), 2.32 (2H, m), 1.29 (3H, s), 1.28 (3H, s), 1.24 (3H, s), 1.22 (3H, s), 1.21 (3H, s), 1.19 (3H, s), 1.18 (3H, s). ^{13}C NMR ($CDCl_3$) δ 164.36, 163.86, 163.54, 163.38, 162.71, 162.00, 161.04, 153.97, 151.47, 149.42, 146.01, 145.60, 139.61, 139.45, 138.61, 135.60, 134.43, 134.20, 128.47, 128.32, 127.72, 127.16, 126.33, 124.66, 124.22, 122.48, 122.37, 122.30, 118.13, 117.36, 117.13, 116.95, 116.56, 116.36, 100.93, 100.59, 99.21, 98.00, 76.15, 75.89, 75.58, 75.41, 52.79, 28.62, 28.54, 19.72. IR (KBr) ν, (cm^{-1}) 2959, 1740, 1681, 1590, 1536, 1469, 1420, 1356, 1330, 1266, 1217, 1116, 1051, 877, 762. TOF-MS m/z: 1031.39 $[M]^+$, 1053.37 $[M+Na]^+$, 1069.34 $[M+K]^+$.

Hexamer **6a**, from acid **2c** (0.26 g) and amine **4b** (0.22 g). Yield 0.27 g, (80%) (based on amine). Yellow solid. Mp: >250°C. ^{1}H NMR ($CDCl_3$) δ 11.82 (1H, s), 11.61 (1H, s),11.52 (1H, s), 11.36 (1H, s), 11.34 (1H, s), 8.53 (1H, d, J=7.4 Hz), 8.42 (1H, dd, J=7.4, 1.3 Hz), 8.32 (1H, d, J=7.4 Hz), 8.25 (1H, d, J=7.4 Hz), 8.17 (1H, d, J=7.4 Hz), 8.08 (2H, m), 8.03 (1H, d, J=7.4 Hz, 7.99 (1H, d, J=7.4 Hz), 7.82 (1H, d, J=8.0 Hz), 7.66 (1H, d, J=8.0 Hz), 7.49 (1H, s), 7.43 (3H, m), 7.34 (1H, J=8.0 Hz), 7.27 (2H, m), 7.17 (1H, m), 7.13 (1H, s), 6.85 (1H, s), 6.76 (1H, s), 6.55 (1H, s), 6.48 (1H, s), 4.39 (1H, m), 4.19 (2H, m), 4.09 (1H, m), 3.98 (6H, m), 3.76 (2H, m), 3.15 (3H, s), 2.44 (5H, m), 2.25 (1H, m),1.30 (24H, m), 1.18 (12H, m). ^{13}C NMR ($CDCl_3$) δ 163.76, 163.14, 163.07, 162.96, 162.92, 162.59161.97, 161.27, 161.14, 160.79, 160.15, 160.03, 152.98, 150.46, 149.42, 148.76, 145.244, 144.85, 138.78, 138.36, 138.02, 137.62, 134.14, 133.82,

133.72, 133.56, 132.73, 127.95, 127.34, 127.00, 126.88, 126.46, 125.83, 125.77, 123.95, 123.62, 122.65, 122.32, 121.89, 121.71, 121.47, 117.10, 116.90, 116.67, 116.56, 116.34, 115.96, 115.92, 115.64, 100.11, 99.93, 99.75, 98.07, 97.75, 97.72, 75.52, 75.43, 75.38, 75.24, 75.13, 74.74, 52.09, 28.28, 28.19, 28.12, 28.01, 19.48, 19.41, 19.31, 19.22, 19.16. IR (KBr) ν, (cm^{-1}) 2960, 1684, 1540, 1419, 1357, 1264, 1115, 1051, 878, 760. TOF-MS *m/z*: 1515.49 $[M]^+$, 1537.45 $[M+Na]^+$, 1553.45 $[M+K]^+$.

Octamer **8a**, from acid **4c** (0.22 g) and amine **4b** (0.2 g). Yield 0.22 g.(79% based on amine). Yellow solid. Mp: >250°C. ^1H NMR ($CDCl_3$) δ 11.51 (1H, s), 11.38 (1H, s), 11.17 (1H, s), 11.09 (1H, s), 11.01 (1H, s), 10.95 (1H, s), 10.93 (1H, s), 8.32 (1H, dd, *J*=1.3, 6.7 Hz), 8.21 (1H, dd, *J*=1.3, 6.7 Hz), 8.18 (1H, br), 8.16 (1H, s), 8.11 (2H, td, *J*=6.7, 1.3 Hz), 8.03 (1H, dd, *J*=1.3, 6.7 Hz), 7.89 (3H, m), 7.74 (2H, td, *J*=7.4, 1.3 Hz), 7.65 (1H, m), 7.54 (1H, m), 7.43 (1H, t, *J*=8.0 Hz), 7.39 (1H, t, *J*=8.0 Hz), 7.29 (6H, m), 7.15 (1H, m), 7.06 (1H, s), 7.02 (1H, s), 6.99 (1H, t, *J*=8.0 Hz), 6.67 (1H, s), 6.62 (1H, s), 6.55 (1H, s), 6.51 (1H, s), 6.37 (1H, s), 6.13 (1H, s), 3.90 (12H, m), 3.67 (4H, m), 3.00 (3H, s), 2.52 (2H, m), 2.35 (5H, m), 2.19 (1H, m), 1.36 (12H, m), 1.20 (36H, m). ^{13}C NMR ($CDCl_3$) δ 163.71, 162.80, 162.74, 162.71, 162.62, 162.59, 162.40, 162.31, 161.86, 161.00, 160.77, 160.52, 160.03, 159.71, 159.26, 159.24, 152.99, 149.89, 149.14, 149.08, 148.79, 148.65, 148.09, 144.94, 144.63, 138.64, 138.60, 138.06, 137.96, 137.70, 137.55, 137.51, 137.32, 134.08, 133.55, 133.18, 132.78, 132.64, 127.83, 127.50, 126.87, 126.75, 126.25, 125.74, 125.72, 125.62, 125.49, 123.71, 123.48, 122.53, 122.32, 122.24, 121.54, 121.36, 121.24, 117.23, 116.89, 116.75, 116.64, 116.61, 116.29, 116.17, 116.02, 115.98, 115.92, 115.85, 115.78, 115.46, 99.92, 99.77, 99.49, 99.11, 98.62, 97.82, 97.59, 97.40, 75.46, 75.31, 75.28, 75.22, 75.15, 74.97, 74.65, 51.92, 28.19, 28.16, 28.13, 28.11, 28.07, 28.05, 28.01, 27.91, 19.58, 19.55, 19.51, 19.47, 19.43, 19.36, 19.34, 19.29, 19.22, 19.20, 19.13. IR (KBr) ν, (cm^{-1}) 2960, 1684, 1539, 1469, 1419, 1357, 1331, 1264, 1212, 1114, 1053, 878, 817, 759. TOF-MS *m/z*: 1999.73 $[M]^+$, 2021.73 $[M+Na]^+$, 2037.70 $[M+K]^+$.

Decamer **10a**, from acid **2c** (10 mg) and amine **8b** (17 mg) was prepared as the other oligomers, but toluene at 80°C overnight was used instead of CH_2Cl_2 at ambient temperature. Yield 6 mg (29%). Mp: >250°C. Yellow solid. ^1H NMR ($CDCl_3$) δ 11.33 (1H, s), 11.23 (1H, s), 10.96 (1H, s), 10.90 (1H, s), 10.79 (1H, s), 10.70 (1H, s), 10.66 (1H, s), 10.63 (1H, s), 10.60 (1H, s), 8.28 (1H, d, *J*=7.4 Hz), 8.10 (1H, d, *J*=7.4 Hz), 8.02 (6H, m), 7.78 (2H, t, *J*=7.4 Hz), 7.68 (2H, m), 7.52 (1H, d, *J*=7.4 Hz), 7.35 (4H, m), 7.20 (12H, m), 6.96 (3H, m), 6.66 (1H, s), 6.51 (1H, s), 6.37 (2H, d), 6.31 (1H, s), 6.12 (1H, s), 6.10 (1H, s), 6.05 (1H, s), 4.05 (5H, m), 3.89 (8H, m), 3.75 (4H, m), 3.62 (3H, m), 2.93 (3H, s), 2.31 (10H, m), 1.17 (60H, m). IR (KBr) ν, (cm^{-1}) 2961, 1684, 1541, 1458, 1418, 1356, 1262, 1210, 1112, 1052, 877, 816, 758. TOF-MS *m/z*: 2483.61 $[M]^+$, 2505.58 $[M+Na]^+$, 2521.57 $[M+K]^+$.

7.2. X-Ray diffraction analysis

The structures of **1a**, **1b**, **1c**, **1d** and **2a** were determined by single-crystal X-ray diffraction techniques. For the first four structures, the data were collected on a CAD4 Enraf–Nonius diffractometer with graphite monochromatized Cu K_α radiation. The cell parameters were determined by least-squares from the setting angles for 25 reflections. An empirical absorption correction was applied. The data were also corrected for Lorentz and polarization effect. The crystals of **2a** are mechanically fragile as well as unstable in air. During the X-ray exposures, they were sealed with part of the mother liquor in a Lindemann-glass capillary. The single crystal was mounted on a Bruker–Nonius κ-CCD diffractometer with graphite monochromatized Mo K_α radiation (0.71073 Å). The data collection was based on ϕ-scans completed by ω-scans. The final unit cell was determined on the basis of all the collected frames. The data reduction was performed using the COLLECT software (Nonius, 1998). The positions of non-H atoms were determined by the program SHELXS 87 and the position of the H atoms were deduced from coordinates of the non-H atoms and confirmed by Fourier Synthesis. H atoms were included for structure factor calculations but not refined.

Acknowledgements

This work was supported by the Universities of Bordeaux I and of Bordeaux II, by the Centre National de la Recherche Scientifique (predoctoral fellowship to C. D.), and by the Ministère de la Recherche (post-docotral fellowship to H. J.).

References

1. Gellman, S. H. *Acc. Chem. Res.* **1998**, *31*, 173–180.
2. Cheng, R. P.; Gellman, S. H.; DeGrado, W. F. *Chem. Rev.* **2001**, *101*, 3219–3232.
3. Hill, D. J.; Mio, M. J.; Prince, R. B.; Hughes, T. S.; Moore, J. S. *Chem. Rev.* **2001**, *101*, 3893–4012.
4. For recent examples of structural studies: LePlae, P. R.; Fisk, J. D.; Porter, E. A.; Weisblum, B.; Gellman, S. H. *J. Am. Chem. Soc.* **2002**, *124*, 6820–6821. Porter, E. A.; Wang, X.; Schmitt, M. A.; Gellman, S. A. *Org. Lett.* **2002**, *4*, 3317–3319. Etezady-Esfarjani, T.; Hilty, C.; Wüthrich, K.; Rueping, M.; Schreiber, J.; Seebach, D. *Helv. Chim. Acta* **2002**, *85*, 1197–1209. Cheng, R. P.; DeGrado, W. F. *J. Am. Chem. Soc.* **2002**, *124*, 11564–11565. Glattli, A.; Daura, X.; Seebach, D.; van Gunsteren, W. F. *J. Am. Chem. Soc.* **2002**, *124*, 12972–12978. Seebach, D.; Brenner, M.; Rueping, M.; Jaun, B. *Chem. Eur. J.* **2002**, *8*, 573–584.
5. For examples of potential biological applications of these peptide mimics: Porter, E. A.; Weisblum, B.; Gellman, S. H. *J. Am. Chem. Soc.* **2002**, *124*, 7324–7330. Raguse, T. L.; Porter, E. A.; Weisblum, B.; Gellman, S. H. *J. Am. Chem. Soc.* **2002**, *124*, 12774–12785. Porter, E. A.; Wang, X.; Lee, H.-S.; Weisblum, B.; Gellman, S. H. *Nature* **2000**, *404*, 565. Hamuro, Y.; Schneider, J. P.; DeGrado, W. F. *J. Am. Chem. Soc.* **1999**, *121*, 12200–12201. Werder, M.; Hauser, H.; Abele, S.; Seebach, D. *Helv. Chim. Acta* **1999**, *82*, 1774–1783.
6. Hamuro, Y.; Geib, S. J.; Hamilton, A. D. *J. Am. Chem. Soc.* **1996**, *118*, 7529–7541.
7. Hamuro, Y.; Geib, S. J.; Hamilton, A. D. *J. Am. Chem. Soc.* **1997**, *119*, 10587–10593.

8. Singha, N. C.; Sathyanarayana, D. N. *J. Mol. Struct.* **1997**, *403*, 123–135.
9. (a) Berl, V.; Huc, I.; Khoury, R. G.; Lehn, J.-M. *Chem. Eur. J.* **2001**, *7*, 2798–2809. (b) Huc, I.; Maurizot, V.; Gornitzka, H.; Léger, J.-M. *Chem. Commun.* **2002**, 578–579. (c) Berl, V.; Huc, I.; Khoury, R. G.; Krische, M. J.; Lehn, J.-M. *Nature* **2000**, *407*, 720–723. (d) Berl, V.; Huc, I.; Khoury, R. G.; Lehn, J.-M. *Chem. Eur. J.* **2001**, *7*, 2810–2820.
10. Delnoye, D. A. P.; Sijbesma, R. P.; Vekemans, J. A. J. M.; Meijer, E. W. *J. Am. Chem. Soc.* **1996**, *118*, 8717–8718.
11. Gong, B. *Chem. Eur. J.* **2001**, *7*, 4337–4342. Zhu, J.; Parra, R. D.; Zeng, H.; Skrzypczak-Jankun, E.; Cheng Zeng, X.; Gong, B. *J. Am. Chem. Soc.* **2000**, *122*, 4219–4220.
12. Corbin, P. S.; Zimmerman, S. C. *J. Am. Chem. Soc.* **2000**, *122*, 3779–3780. Corbin, P. S.; Zimmerman, S. C.; Thiessen, P. A.; Hawryluk, N. A.; Murray, T. J. *J. Am. Chem. Soc.* **2001**, *123*, 10475–10488.
13. Garric, J.; Léger, J.-M.; Grelard, A.; Ohkita, M.; Huc, I. *Tetrahedron Lett.* **2003**, *44*, 1421–1424.
14. Nowick, J. S.; Lam, K. S.; Khasanova, T. V.; Kemnitzer, W. E.; Maitra, S.; Mee, H. T.; Lui, R. *J. Am. Chem. Soc.* **2002**, *124*, 4972–4973, and references therein. Zeng, H.; Yang, X.; Flowers, R. A.; Gong, B. *J. Am. Chem. Soc.* **2002**, *124*, 2903–2910.
15. For examples of biological applications of aromatic oligoamide foldamers: Tew, G. N.; Liu, D.; Chen, B.; Doerksen, R. J.; Kaplan, J.; Carroll, P. J.; Klein, M. L.; DeGrado, W. F. *Proc. Natl. Acad. Sci. (USA)* **2002**, *99*, 5110–5114. Ernst, J. T.; Becerril, J.; Park, H. S.; Yin, H.; Hamilton, A. D. *Angew. Chem. Int. Ed.* **2003**, *42*, 535–539.
16. For a preliminary communication about these oligomers, see: Jiang, H.; Léger, J.-M.; Huc, I. *J. Am. Chem. Soc.* **2003**, *125*, 3448–3449.
17. Peet, N. P.; Baugh, L. E.; Sunder, S.; Lewis, J. E. *J. Med. Chem.* **1985**, *28*, 298–302.
18. Wender, P. A.; Jessop, T. C.; Pattabiraman, K.; Pelkey, E. T.; VanDeuse, C. L. *Org. Lett.* **2001**, *3*, 3229–3232.
19. The distance is between the two heavy atoms, and the angle is the *N*–H···(N/O) angle.
20. Matsuda, K.; Stone, M. T.; Moore, J. S. *J. Am. Chem. Soc.* **2002**, *124*, 11836–11837.
21. For a discussion about a similar helix inversion mechanism, see: Ohkita, M.; Lehn, J.-M.; Baum, G.; Fenske, D. *Chem. Eur. J.* **1999**, *5*, 3471–3481.